International Journal of Physics, 2018, Vol. 6, No. 3, 85-92
Available online at http://pubs.sciepub.com/ijp/6/3/4

DOI:10.12691/ijp-6-3-4

Experimental Study of Electrical Resistivity to Rock Fracture Intensity and Aperture Size

Amadu Casmed Charles[1,*], Gawu Simon K.Y[2], Abanyie K. Samuel[1]

[1]Earth and Environmental Sciences Department, University for Development Studies (UDS), P. O. Box 20, Navrongo, Ghana
[2]Department of Geological Engineering, Kwame Nkrumah University of Science and Technology (KNUST), Kumasi, Ghana
*Corresponding author: camadu@uds.edu.gh

Abstract Fracture geometric characteristics (FGC) such as fracture intensity, fracture network connectivity and aperture distribution are crucial features controlling the hydraulic and geotechnical properties of rock formations. Geophysical methods have been used to detect contrast in subsurface material. The Electrical Resistivity (ER) method is one of such methods. The method was applied in an experimental test to investigate ER response with varying fracture intensity I_f and aperture size *Aper width* in an experimental set-up at Kwame Nkrumah University of Science and Technology (KNUST, Kumasi, Ghana, geotechnical laboratory. The concepts of electrical resistivity variation with rock mass fracture intensity, and aperture were used to obtained experimental data. ER profiles, each measuring 0.9 m long were recorded using 4 electrodes deployed using the Dipole-dipole, Wenner and Schlumberger configurations from the experimental setup. To quantify the relationship between apparent resistivity and fracture intensity, scatter-plots were drawn with apparent resistivity as the abscissa and fracture intensity as well as aperture width as ordinate. There were strong positive linear and regressive correlations between ρa and fracture intensity. Mathematical relationships are established that relate the ER and fracture intensity, and ER with aperture width. The highest coefficient of determination R^2 of 0.924 was represented for best fit equation, $\rho_a = 1576.9 \ln f_n - 0.405$, for relationship between apparent resistivity and fracture intensity. For aperture width, the best fit model was given a logarithmic relation as ρ_a =-465.46(Aperture width)^2 +4880.5(Aperture width)+1295.5. The study demonstrates the potential usefulness of the ER approach in rock fracture characterisation investigations, which is economic, efficient and less time consuming compared to other methods, of subsurface fracture characterization such core drilling.

Keywords: *geophysics, rock block samples, rock fracture intensity, electrical resistivity experiments*

Cite This Article: Amadu Casmed Charles, Gawu Simon K.Y, and Abanyie K. Samuel, "Experimental Study of Electrical Resistivity to Rock Fracture Intensity and Aperture Size." *International Journal of Physics*, vol. 6, no. 3 (2018): 85-92. doi: 10.12691/ijp-6-3-4.

1. Introduction

The characterisation of shallow subsurface material and the spatial variability at large scale is a crucial issue in many research studies and fields of application, ranging from agriculture, mineral and petroleum exploration, geology, to civil and environmental engineering. Investigations on the movement of fluid and contaminants through rock mass and the factors that control such movements are of great concerns in the hydrogeological field.

Fracture properties such as intensity, fracture network connectivity and aperture size distribution are crucial features controlling the hydraulic and geotechnical properties of rock formation. In this experimental study the focus is on the response of electrical resistivity to fracture density and variation in aperture width.

Information on subsurface fracture properties are often obtained traditionally through site characterisation which rely on sparse network of intrusive sampling points which consist of test pitting, coring and monitoring wells [1,20]. Electrical resistivity methods have a wide range of applications. It has been used extensively in the search for suitable groundwater sources [2], for soil characterisation [3], landslide modelling [4], monitoring of soil moisture content [5] and detecting salt–water intrusion [6] among others.

Although these techniques have been widely implemented at various sites, there are a number of limitations in the use of these techniques. These direct observation approaches of charactering the subsurface are cumbersome, expensive and sometimes impossible. They are time-consuming and suffer from low sampling density, relying on data from a limited number of locations, sometimes, widely spaced [7]. However if properly designed and implemented, geophysical methods are capable of imaging detailed subsurface structures [8].

Studies have shown that geophysical approaches can be used to delineate subsurface geological structures [9,22].

A generalised respond to variations in physical properties of the earth's subsurface including its rocks, fluids and voids have been published [2,8,10,11,12], However, the influence of fracture density or intensity, and variation of fracture aperture and subsequently, variation in volume and concentration of contaminants in fractures is not well understood. The focus of this study is

to help overcome the shortcomings of the conventional approaches in obtaining subsurface fracture properties by advancing electrical resistivity measurement technique.

In this paper, two sets of experimental studies using 6 sets of rock block samples representing different fracture intensity and aperture widths were carried out. Attempts are made separately to discuss the influences of fracture intensity and aperture size on the electrical resistivity of the different rock samples, soil types and attempt to model the relationship between ER and fracture intensity, and also between ER and aperture size.

2. Theoretical Background

The fundamental physical law used in resistivity surveys that governs the flow of electrical current through earth material (soil and/or rock) is Ohm's law The equation for Ohm's law in vector form for current flow in a continuous medium is given by [13,14]:

$$J_C = \sigma E \tag{1}$$

where, σ is the electrical conductivity of the medium, J_c is the current density and E is the electric field intensity.

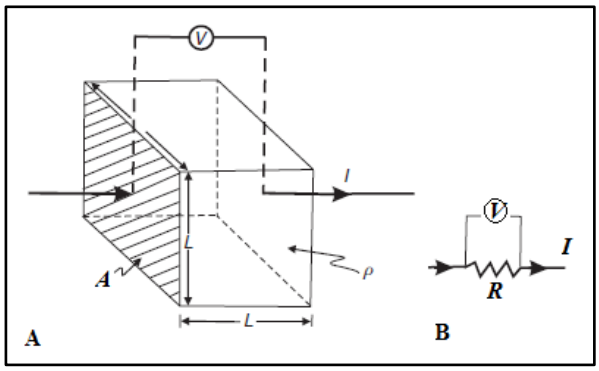

Figure 1. Parameters used in defining resistivity. (A) Definition of resistivity across a block of side length L with an applied current I and potential drop between opposite faces of V. (B) Electrical circuit equivalent, R is a resistor (Modified after Reynold, [2])

The resistivity technique is based on the principle that, when a current, I is passing through an electrically uniform cube of side length L (Figure 1), the material within the cube resists the conduction of electricity through it, resulting in a potential drop, V between opposite faces. The resistance R (Ω) is proportional to the length L (m) of the resistive material and inversely proportional to the cross-sectional area, A (m^2):

$$V = IR \tag{2}$$

where V is voltage, I is current, and R is resistance.

The value of the R varies according to the dimensions of the material such as, length (L) and cross-sectional area (A), measured in meters. The electrical resistivity value, ρ can be acquired by the relationship:

$$\rho = \frac{RA}{L}\Omega m \tag{3}$$

In homogeneous media, the value represents the true resistivity of the medium [14]. However, the geological environment is composed of heterogeneities and therefore the resistivity measures in this case represent a weighted average of true resistivities. This is referred to as the apparent resistivity ρ_a, expressed as:

$$\rho_a = K\left|\frac{\Delta V}{I}\right| \tag{14}$$

where ΔV is the measured potential difference and I is the current passed through the ground.

The arrangement of the current and potential electrodes defines the geometric factor (K), measured in meters, in the determining of resistivity. Thus, the primary objective of generating and measuring an electric potential field is, to determine the spatial distribution of ρ_a (Ω.m) in the subsurface [15].

The process of measuring subsurface resistivity involves, placing four electrodes in the ground in a line at equal spacing, applying a measured direct current (DC) or low frequency alternating current (AC) to the outer two electrodes, and measuring the AC voltage between the inner two electrodes. A measured resistance is calculated by dividing the measured voltage by the measured current. This resistance is then multiplied by the geometric factor that depends on the spacing (a) between each electrode (Figure 2) to determine the apparent resistivity (ρa). the geometric factor for the Wenner array is, K = 2πa, and K = (n -1)(n +1)πa/2 for the Schlumberger. For the dipole–dipole configuration, the current electrodes AB and the potential electrodes MN have the same spacing a but the two pairs are widely separated by a distance na, where n >> 1. The geometric factor for the dipole–dipole array is, K = πn(n + 1)(n + 2)a.

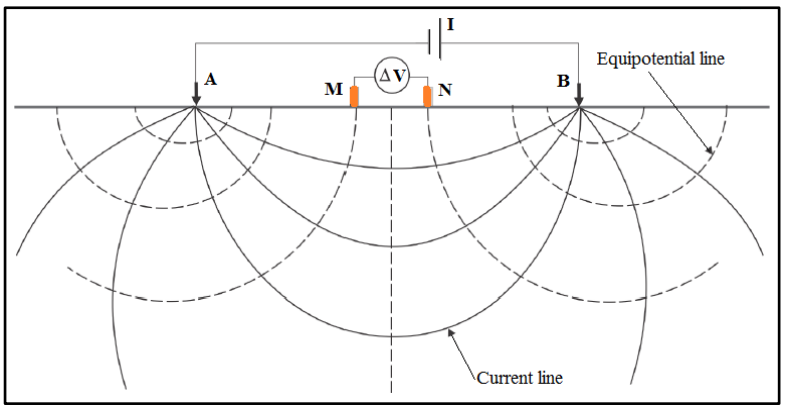

Figure 2. Field Acquisition of Resistivity data (Modified from [10])

3. Methodology

The experimental procedures and methodologies employed in this study to investigate ER response to fracture intensity and aperture width are presented in detail in the following sections.

3.1. Experiment System and Sample Preparation

The experimental work was in two parts, profiling of electrical response to: (1) fracture intensity, and, (2) aperture variation. Prior to the experimental exercise, model rock blocks were prepared to be used as replicas of fractures, fracture spacing, intensity, and aperture variations.

3.1.1. Model Blocks Preparation

From field outcrops and core observations, typical fractures in tight sedimentary and crystalline rocks, consists of fractures with aperture width between 0.1 to 10.0 mm, and filled with air, water, clay material, quartz or other cementing material [16]. To investigate the effect of fracture density and aperture variation on ER response, a number of rock model blocks were prepared. The rock blocks were obtained from a quarry site near Ablekuma in the Greater Accra Region, Ghana. The rocks are lightgrey, fine-medium grained, metaporphosed quartzite of the Togo structural units (TSU) [17]. They are composed of quartz, apatite, sericite and alkaline-feldspar. The rocks were selected for sample preparation based on their grain size, quality (competent and unweathered) and low matrix permeability. This was done mainly with the view that, flow and transport takes place principally only through the fractures and not the matrix [18,19].

The rock blocks were trimmed into regular geometrically defined samples at the Geotechnical Laboratory of Kwame Nkrumah University of Science and Technology (KNUST). Due to challenges in cutting specimen rock blocks, the largest rock block, which was also used as intact rock sample block was 35 cm x 20 cm x 30 cm. The sample rock block IDs and their dimensions are presented in Table 1.

3.1.2. Apparatus

An apparatus was constructed for measuring the horizontal electrical resistivity of intact and representative fractured rock. The apparatus consists of a wooden case of dimension 90 x 22 x 27 cm, four copper electrodes, MiniRes Ultra40 resistivity meter, connecting cables (Figure 3), calipers, and measuring tape. The wooden case is an electrical insulator (electrical resistivity ~ 1.00×10^{14} to 1.00×10^{16} ohm-m, (Anon 2018).

3.1.3. Experimental Setup and Apparent Measurement Procedures

Electrical resistivity investigation was in two parts, profiling of electrical response to: 1) fracture intensity, to infer the variations of resistivity along horizontal as fracture intensity increases, and 2) aperture width variation. Apparent resistivity measuring procedure involves, spreading fine grained soil at the bottom (up to 10 cm thick), placing the rock block or blocks sample in the wooden case (at the central portion), spreading fine grained soil top of the rock block up to a thickness of 15 cm and driving the electrodes into the soil on top of the rock block sample.

To collect resistivity data using the MiniRes Ultra40 imaging system, the electrodes were deployed along an array in the Dipole-Dipole, Wenner, and Sclumberger configurations. For a typical measurement, the MiniRes meter reading, together with the spacing of the electrodes were recorded. If the electrodes were spaced at uniform intervals $\boldsymbol{a}$ along the line, then the apparent resistivity is calculated by the relation:

$$\rho_a = 2\pi \mathbf{a}\rho \quad (4)$$

where, ρ is the resistance read on the MiniRes.

One complete profile was performed for each sample.

Table 2 presents the combinations of the different blocks and the resulting number of fractures and fracture area.

Table 1. Sample Rock Block IDs and their Dimensions

Rock block ID.	Fracture series	Dimension (length, width and height) cm	Number of pieces	Comments
1	A	30 x 20 x 25	1	Used as intact rock
2	B	15 x 20 x 25	2	Used for single fracture and aperture variation
3	C	12.5 x 20 x 25	2	For two fractures
4	D	10 x 20 x 25	2	For three fractures
5	E	7.5 x 20 x 25	2	For four fractures
6	F	5.0 x 20 x 25	6	For five fractures
Total number of pieces			15	

Table 2. Experimental Arrangement for Fracture Intensity

Experiment No.	Number of fractures	Total fracture area (cm^2)	Comments
1	0		Intact rock
2	1	950	Single fracture
3	2	1900	2 Fractures
4	3	2850	3 Fractures
5	4	3800	4 Fractures
6	5	4750	5 Fractures

A B

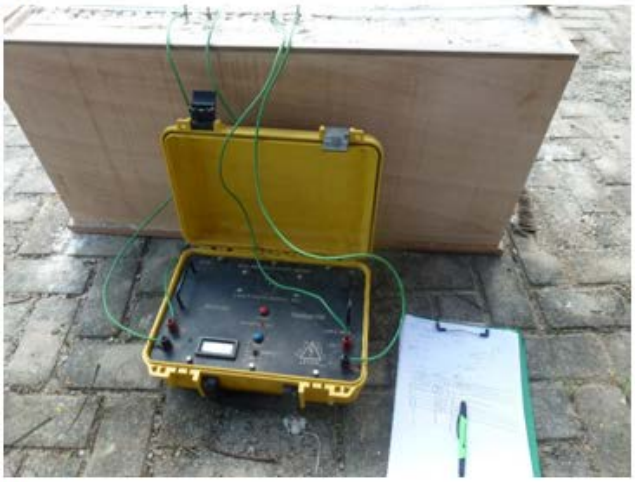

C

Figure 3. Experimental system and procedure used for studying Effect of Fracture Intensity and Aperture Size. (A) Rock blocks (B) Series of rock blocks use as fracture samples, (C) Experimental setup (Dipole-Dipole configuration)

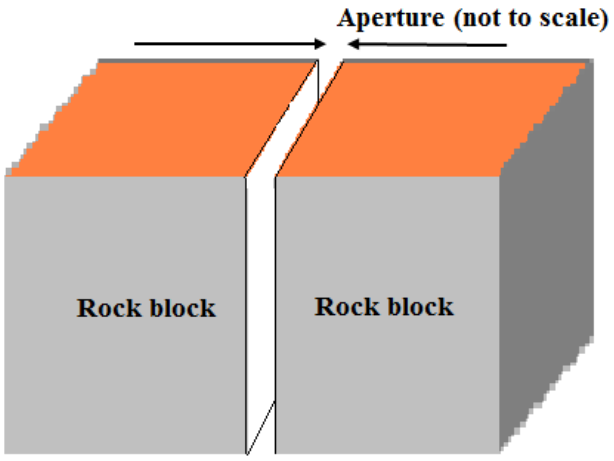

Figure 4. Design for Study of Variation of Aperture Size

Table 3. Electrical Response to Aperture Size Variation

Experiment No.	Aperture size (mm)	Fracture surface area (cm^2)	Comment
1	0.2	950	Created by inserting 2 plain A-4 sheets
2	0.5	950	Created by inserting 4 plain A-4 sheets
3	1.0	950	Created by inserting 8 plain A-4 sheets
4	2.0	950	Created by inserting 16 plain A-4 sheets
5	4.0	950	Created by inserting 32 plain A-4 sheets
6	6.0	950	Created by inserting 48 plain A-4 sheets

For aperture variation, the arrangement of electrodes and current flow system remain unchanged except that, in this case, two rock blocks (15 x 20 x 25 cm) were used (Figure 4), and the spacing between the faces in contact varied from 0.2 mm to 10 mm (Table 3). Measurements of change in aperture was done using the calipers. A pieces of A-4 paper was placed in between the spacing to avoid the opposite fracture faces coming into contact or being filled by the soil particles. Resistivity data was collected using the MiniRes Ultra40 imaging system. Electrodes were deployed along an array in the Schlumberger configuration.

There were 6 experiments in total and, for each experiment, current flow data were recorded.

3.1.4. Data Modelling and Interpretation

Fundamental principle to all resistivity methods is the concept that, current (I) can be impressed into the ground and the effects of the current within the ground can be measured (Van Nostrand and Cook, 1996). The apparent resistivity ρ_a, as measured by the electrical imaging (EI) system is, the product of the entire rock block under the soil cover responding to the impressed current. Due to the presence of fractures, the rock block is no more homogeneous, it is important therefore, to model the apparent resistivities at discrete locations in order to make a more quantitative interpretation. Inverse modelling was performed using RES2DINV^{TM} software 21] to produce a two dimensional resistivity model based on the applied resistivity data.

Following the inverse modelling, the EI electrostructural information was used to interpret features of interest (geometry of the rock blocks, effects of the fractures and aperture size).

4. Results and Discussions

4.1. Effect of Fracture Intensity on Apparent Resistivity

The resistivity profiles defined the geometry of rock block sample (Figure 5) and indicates medium range resistivity values 800 to 1000 Ohm-m).

Figure 5 shows some of the resistivity imaging profiles acquired across the wooden case with rock samples located within the central portion. For the samples studied, the apparent resistivity ranged from about 1,200 Ohm-m (intact rock) to about 12,500 Ohm-m, at the highest fracture intensity (5 fractures) (Table 4). As expected, fracture surface area increased with the increase of number of fractures.

Maximum and minimum values of ρ_a were 1000-1300 and 10000-12500 Ωm respectively.

Changes in ρ_a values indicates the variation of electrical response. To quantify the relationship between apparent resistivity and fracture intensity, a scatter-plot (Figure 6) was drawn with apparent resistivity as the abscissa and fracture intensity as ordinate.

The aim of this part of the experimental work was to investigate effects of fractures on apparent resistivity. Thus, only measured apparent resistivity values for fractured rock samples were plotted and modelled.

The 2D images of the Schlumberger array approach resistivity data appear to define the geometry of the rock blocks much better than the Wenner and Dipole-Dipole resistivity data. The Dipole-Dipole method was much time consuming.

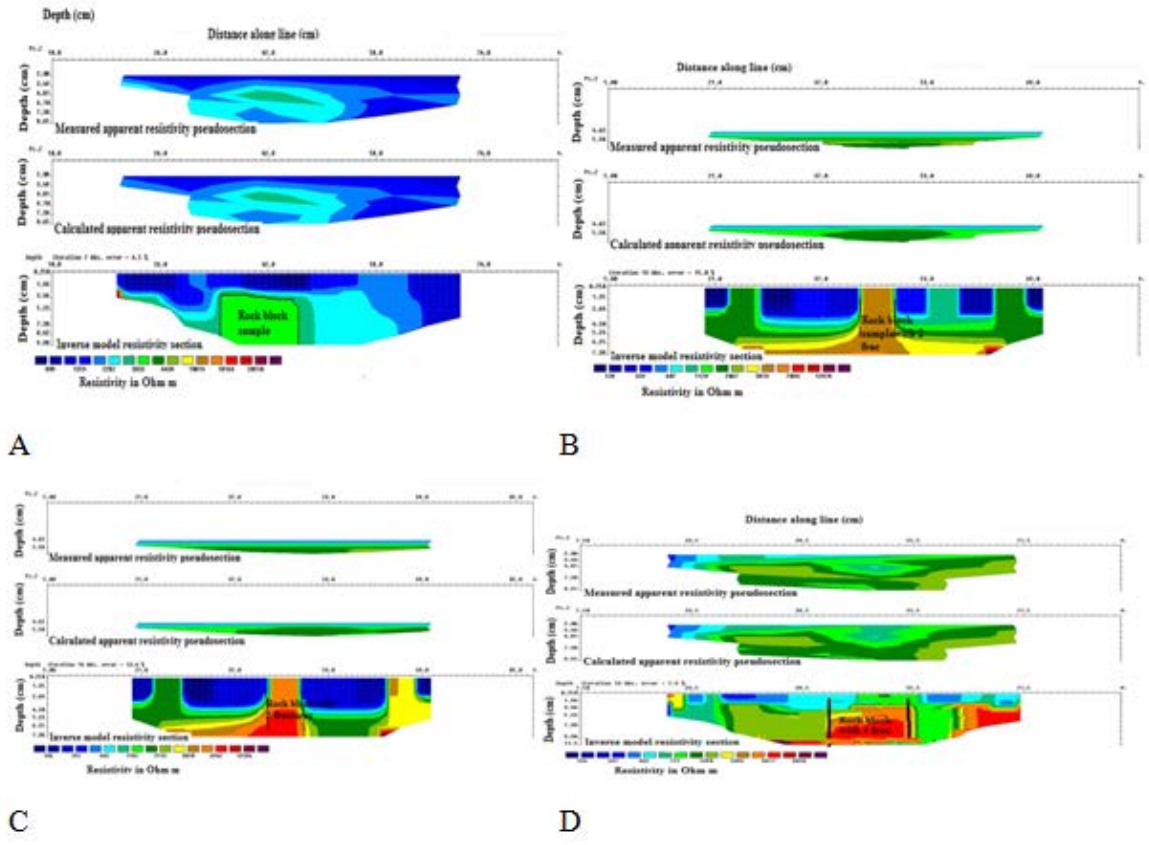

Figure 5. Samples of 2D Apparent Resistivity Pseudosections of the Laboratory Experiments. (A) Sample block with 2 Fractures, (B) Block with 2 Fractures, (C) Block with 4 Fracture, (D) Block with 5 Fractures

Table 4. Summary of measured apparent resistivity for fractured rock samples

Sample ID	1	2	3	4	5	6
Number of fractures	0	1	2	3	4	5
Apparent resistivity (Ohm-m)	1120	2500	3813	3902	9500	12000

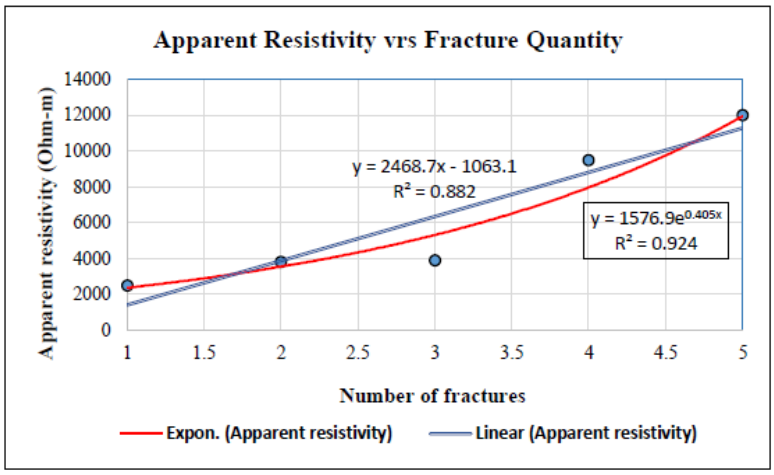

Figure 6. Apparent resistivity versus fracture quantity

There were strong positive linear and regressive correlations between ρa and fracture intensity.

With increasing number of fractures, the apparent resistivity increases in a power law relationship (exponential distribution) as:

$$y = 1576.9e^{0.405x} \quad (5)$$

With coefficient of determination, $R^2 = 0.924$, i.e.

$$\rho_a = 1576.9\ln f_n - 0.405 \quad (6)$$

Where ρ_a is apparent resistivity, and f_n is the number of fractures

Generally the relationship between apparent resistivity and fracture show strong linear and regression, however the highest coefficient of determination R^2 of 0.924 was represented in Equation 5.

The probability density function of the exponential distribution involves a parameter, which is a positive constant λ whose value determines the density function's location and shape.

$$f(x) = \begin{cases} \lambda e^{-\lambda x} & \text{for, } x > 0 \\ 0, & \text{for, } x \le 0 \end{cases}$$

where λ is the value at which plot of the probability density function intercepts the y-axis.

4.1.1. Effect of Aperture Size on Apparent Resistivity

Figure 7 shows the electrical image across the vertical fracture with aperture of 6 mm between the comparatively lower resistivity quartzite rock block.

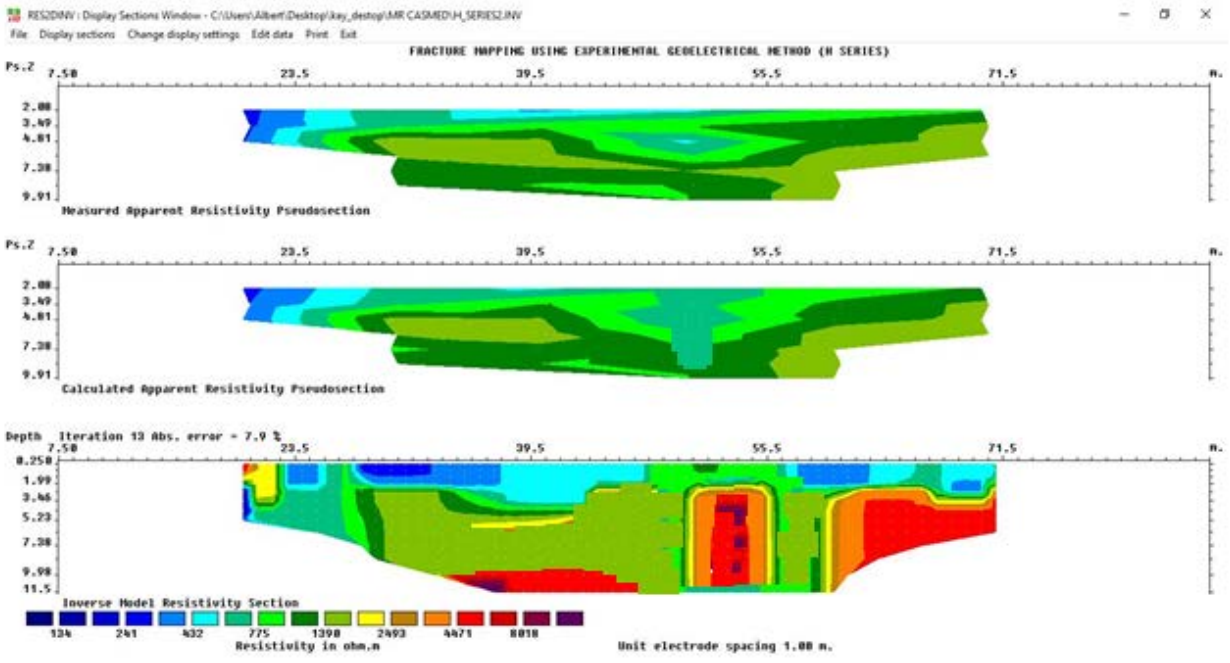

Figure 7. Electrical image across the vertical fracture with aperture of 6 mm between the comparatively lower resistivity quartzite rock block

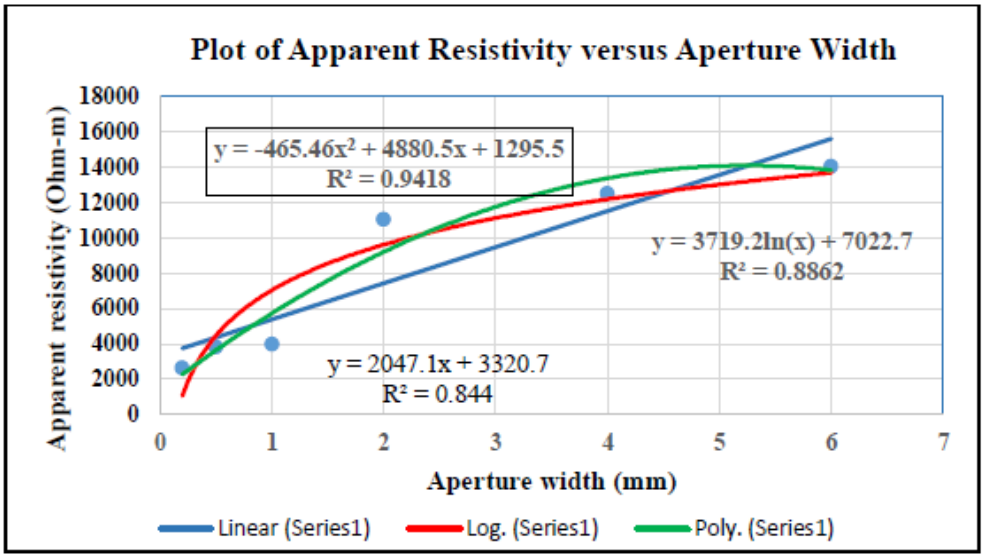

Figure 8. Apparent resistivity versus Aperture Width

Table 5. Summary of measured apparent resistivity for varying aperture size

Sample ID	1	2	3	4	5	6
Aperture size (mm)	0.2	0.5	1	2	4	6
Apparent resistivity (Ohm-m)	2620	3800	3950	11050	12500	14050

For the samples studied, the apparent resistivity ranged from about 2620 Ohm-m (intact rock) to about 14050 Ohm-m. Measured apparent values where plotted for model construction. Table 5 is a summary of the experimental results.

The aim of this part of the experimental work was to investigate effects of fractures on apparent resistivity. Thus, only measured apparent resistivity values for fractured rock samples were plotted and modelled.

The best fit model was given a logarithmic relation as follows_

$$y = -465.46x^2 + 4880.5x + 1295.5 \quad (7)$$

i.e.

$$\rho_a = -465.46(\text{Aperture width})^2 + 4880.5(\text{Aperture width}) + 1295.5 \quad (8)$$

Where ρ_a is apparent resistivity.

The resistivity data also indicate a well-defined high resistivity anomaly at central portion of the rock block samples, which could be interpreted as wood and near to an airfilled apace.

The effects of fractures and aperture size on apparent resistivity in fractured crystalline rocks have been investigated. The laboratory measurement results indicates, apparent resistivity increases with increase in fracture intensity and aperture size and are modelled with a power laws, suggesting that, fractures and fractured zones can be detected by locating the highest resistivity contrast regions.

This experimental investigation provides further evidence for the identification of rock contrasts using electrical resistivity approach reported by, Sandberg et al., 2002; Skinner and Heinson, [9], and Falgas et al., 2011.

Fractures and fractured zones often constitute a discontinuity creating an anomaly within an otherwise homogeneous rockmass. They can be identified geophysically by the contrasting properties of the presence of a fracture or fracture zone, irrespective of the rock types.

5. Conclusions

The experimental results indicates that the measurements of electrical resistivity depend on electrical heterogeneity and that variations in the signal were detectable, even at the laboratory scale. For each rock sample with the same rock type and infill material, apparent resistivity increases as fracture intensity and aperture width increases.

The measurements enabled a relationship between electrical resistivity and fracture intensity on one hand, and resistivity and aperture width to be established. The mathematical models established in the investigation can be explored to aid future investigation into field applicability of ER methods to characterise fracture density and aperture size distribution in near-surface crystalline rocks.

References

[1] Griffin, T. W. and Watson, K. W. (2002). A Comparison of Field Techniques for Confirming Dense Nonaqueous Phase Liquids. Groundwater Monitoring and Remediation, Vol. 22, Issue 2. pp 48-59.

[2] Reynolds, J. M. (2011). An Introduction to Applied and Environmental Geophysics. New York, NY: Wiley-Blackwell.

[3] Kumari S, Israil M, Mittal S, Rai J (2009) Soil characterization using electrical resistivity tomography and geotechnical investigations. J Appl Geophys. 67(1): 74-79.

[4] Piegaria, E., Cataudella, V., Di Maio, R., Milano, L., Nicodemi, M. and Soldovieri, M. G. (2009). Electrical resistivity tomography and statistical analysis in landslide modelling: a conceptual approach. J Appl Geophys 68(2): 151-158.

[5] Brunet, P., Rémi, C., Christophe, B. (2010). Monitoring soil water content and deficit using electrical resistivity tomography (ERT) – A case study in the cavennes area, France. J Hydrol. 380(1-2): 146-153.

[6] de Franco, R., Biella, G., Tosi, L., Teatini, P., Lozej, A., Chiozzotto, B., Giada M., Rizzetto, F., Claude, C., Mayer, A., Bassan, V. and Gasparetto-Stori, G. (2009). Monitoring the saltwater intrusion by time lapse electrical resistivity tomography: the chioggia test site (Venice Lagoon, Italy). J Appl Geophys 69(3-4):117-130.

[7] Boadu, F. K., and Long, L. T. (1996), Effects of fractures on seismic-wave velocity and attenuation. Geophys. J. Int., 127, pp. 86-110.

[8] Loke, M. H. (2001). Electrical Imaging Surveys for Environmental and Engineering Studies. A Practical Guide to 2-D and 3-D Surveys. RES2DINV Manual. IRIS Instruments. www.iris-intruments.com.

[9] Skinner, D., Heinson, G., (2004). A comparison of electrical and electromagnetic methods for the detection of hydraulic pathways in a fractured rock aquifer, Clare Valley, South Australia. Hydrogeol. J. 12, 576-590.

[10] Telford, W. M. W.; Gedart, L. P.; Sheriff, R. E. (1990) Applied Geophysics. London, UK: Cambridge University Press - Second Edition. 792 p.

[11] Singh, D. N., Kuriyan, S. J., Chakravarthy, M. (2001). A generalized relationship between soil electrical and thermal resistivities. Exp. Thermal Fluid Sci. 25 (3-4), 175-181.

[12] Lowrie, W. (1997). Fundamental of geophysics, Cambridge University Press, Switzerland, 254 pp.

[13] Tsourlos, P. (1995). Modeling, Interpretation and Inversion of Multi-electrode Resistivity Data. D.Phil. Thesis, University of York, 315 pp.

[14] Everett, M. E. (2013). Near-Surface Applied Geophysics. Cambridge University Press, 442 p.

[15] Vogelsang, D (1995). Environmental Geophysics: A practical guide. Berlin: Springer.173p.

[16] Amadu, C. C. Foli, G. and Abanyie, S. (2017). Rock Fracture Characterization for Solid Waste Disposal Site Selection: A Case from Sites in the Accra-Tema Area, SE Ghana. *World Journal of Environmental Engineering*, Vol. 5, No. 1, 7-16.

[17] Kesse, G. O. (1985). The mineral and rock resources of Ghana. A. A. Balkema Publishers, The Netherlands, 610p.

[18] Brace, W. F. (1980). Permeability of crystalline and argillaceous rocks, Int. J. Rock. Mech. Min. Sci. Geomech. Abstr. 17, 241-251.

[19] Brown, S. R. (1989). Transport of fluid and electric current through a single fracture, J. Geophys. Res., 94, 9429-9438.

[20] Kearey, P. and Brooks, M. (1991). An Introduction to Geophysical Exploration: Blackwell Scientific. 254 pp.

[21] Loke, M. H. and Barker, R. D. (1996). Rapid least squares inversion of apparent resistivity pseudosections by a quasi-Newton method. Geophys. Prospect, 44, 131-152.

[22] Slatera, L., Binley, A., Versteegc, R., Cassiani, G., Birkend, R and Sandberg, S. (2002). A 3D ERT study of solute transport in a large experimental tank. Journal of Applied Geophysics. Volume 49, Issue 4, pp. 211-229.